Journal of RAMAN SPECTROSCOPY

Al-Si ordering in albite: a combined single-crystal XRD and Raman spectroscopy study

Journal:	*Journal of Raman Spectroscopy*
Manuscript ID	JRS-18-0153.R3
Wiley - Manuscript type:	Research Article
Date Submitted by the Author:	n/a
Complete List of Authors:	Tribaudino, Mario; Dipartimento di Scienze Chimiche, della Vita e della Sostenibilità Ambientale Gatta, Giacomo; Dipartimento di Scienze della terra Aliatis, Irene; University of Parma, Physic and Earth Sciences Bersani, Danilo; Università degli Studi di Parma, fisica Lottici, Pier Paolo; University, Physics and Earth Sciences
Keywords:	Al-Si order, plagioclase, high temperature annealing, X-ray diffraction

. Raman Spectroscopy

Raman spectra of a low albite single crystal were collected during annealing at 1076 °C up to 42 days. At seven annealing stages, the single crystal structure was refined (by X-ray intensity data) in order to calibrate the degree of Al-Si order with peak position and linewidth.
The Raman spectra show a significant broadening with disorder, as well as some slight peak shift. Different peaks show different response to Al-Si disorder.

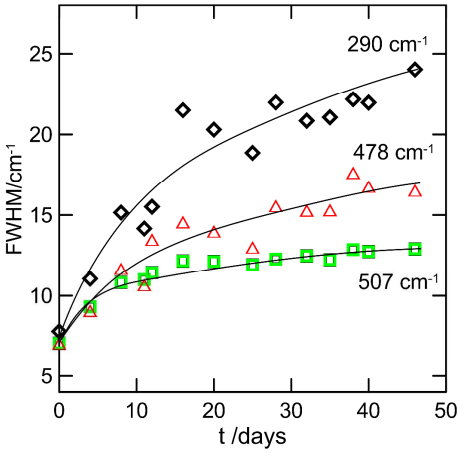

Mario Tribaudino, Diego Gatta, Irene Aliatis, Danilo Bersani and Pier Paolo Lottici

Al-Si ordering in albite: a combined single-crystal XRD and Raman spectroscopy study

Al-Si ordering in albite: a combined single-crystal XRD and Raman spectroscopy study

[1]M. Tribaudino, [2]G.D. Gatta, [3]I. Aliatis, [3]D. Bersani, [3]P.P. Lottici

[1]Department of Chemistry, Life Sciences and Environmental Sustainability, University of Parma, Parco Area delle Scienze 187/a, 43124 Parma, Italy

[2]Earth Sciences Department, University of Milan, via Botticelli 23, 20133 Milan, Italy

[3]Department of Mathematical, Physical and Computer Sciences, University of Parma, Parco Area delle Scienze 7/a, 43124 Parma, Italy

Abstract

Raman spectra of a low albite single crystal were collected during annealing at 1076 °C for up to 46 days. At seven annealing stages, the single crystal structure was refined by X-ray intensity data to determine the degree of Al-Si order using the tetrahedral bond distances. Single crystal X-ray diffraction showed that residuals in the difference-Fourier map of the electron density and atomic displacement parameters of Si, O and, most, Na, increase with Al-Si disorder. The Raman spectra show a significant broadening with disorder, as well as some slight peak shift. Three strong peaks, at 290 cm^{-1} (ν_c), 478 cm^{-1} (ν_b) and 507 cm^{-1} (ν_a) in ordered albite, were examined in further detail. ν_c and ν_b show a red-shift with broadening and Al-Si disorder; ν_a blue-shifts with disorder and shows only a minor broadening. The broadening and shifts in Raman spectra are caused by structural deformation associated with Al-Si disorder. The ν_a peak at 507 cm^{-1} is the least affected by Al-Si disorder, and is suitable to assess compositional changes in plagioclase. The Al-Si order can be determined in albite by the wavenumber difference Δ_{ab} between the two main peaks ν_a and ν_b as:

$$Q_{od}^2 = 9.50(75) - 0.307(25)\Delta_{ab}, \qquad R^2 = 0.94$$

where Q_{od} is an order parameter derived from average tetrahedral Al-O and Si-O bond distances.

1. Introduction

Al-Si order in feldspars has been a fascinating topic until the 1990's [1-4], as an example on how an intracrystalline process can modify the thermodynamics of a system and interact with the elastic behaviour of a mineral. However, in more recent times the interest dropped, as the interest shifted from mineral physics to the applications on natural samples. Ordering and disordering processes have the potential to constrain the thermal history of a feldspar-bearing rock, but the need of crystallographic characterization of the mineral hindered the application of Al-Si order as a petrologic tool. Recent advances in Raman spectroscopy in the calibration of peak position-

linewidth relations with composition, and in the theoretical description of the vibrational modes, now can provide the basis to determine the degree of order of feldspars by Raman methods [5,6]. Raman investigation is quick and simple, it can be done on the same thin section used for optical and SEM-EDS investigations, and, if calibrated, could allow rapid determination of the degree of Al-Si order.

Here we report the first results on albite ($NaAlSi_3O_8$). Albite readily achieves Al-Si disorder within triclinic symmetry by sub-solidus annealing of an ordered crystal. Unit-cell parameters in ordered and disordered albite show significant differences with time and temperature and give a clue to constrain the Al-Si order [2]. The Al-Si order can be measured by unit-cell parameters, on the basis of a single-crystal X-ray diffraction calibration aimed to determine the Al content of the tetrahedral sites from bond distances [7,8].

X-ray diffraction determines the long range order, *i.e.* we can obtain site occupancies by averaging the unit-cells in the examined crystal into an average one. The local ordering, based on nearest neighbour interaction, can be investigated by spectroscopic methods, but few data are to date available. Magic angle spinning nuclear magnetic resonance spectroscopy (MAS NMR) on ^{29}Si, $^{27}A1$ and ^{23}Na in albite revealed a very complex signal with several superimposed peaks [9]. Infrared (IR) spectroscopy experiments [10] correlated peak position, linewidth and amplitude of the IR bands to the degree of order, but the relation between IR and crystal structure was not explored. Moreover, an assignment of the modes to specific vibrations, to relate the spectroscopic results to the crystal structure, was not at the time available.

The IR results suggest that Raman spectroscopy may be able to address the issue of local Al and Si ordering in albite, and in general in plagioclase. Raman spectroscopy enables investigations down to micron size resolution, which allow, in principle, users to determine the changes in Al-Si order through a crystal. To date, few Raman spectroscopy comparisons between the Al-Si ordered low and the Al-Si diosrdered high albite have been explored [11,12]. Freeman et al. [12] found a downshift and broadening of several peaks comparing low and high albite. No study has explored intermediate states, nor have calibrations of albite Al-Si disorder been provided.

In the present study, we analysed the Raman spectra of an albite single crystal annealed to different degree of Al-Si order. The long-range degree of order (Q_{od}) was determined at seven stages of annealing (out of 15) by single crystal X-ray refinement, and was calibrated with Raman peak position and linewidth. Peaks, which are more or less sensitive to Al-Si order, are highlighted, providing the basis for the use of Raman spectra to assess Al-Si order and composition in plagioclase.

2. Experimental methods

2.1 Thermal treatment

The starting material for the experiments is low albite from Minas Gerais (Brazil), with chemical formula $K_{0.02}Ca_{0.01}Na_{0.97}Al_{1.01}Si_{3.00}O_8$ ($Or_{1.79}Ab_{97.29}An_{0.92}$) [5] (the uncertainty in the chemical formula is ±0.01 a.p.f.u.). The albite samples were annealed at 1076 °C in a Lenton Thermal Designs Ltd (LTD) tube furnace (maximum operating temperature 1200 °C). Heating is provided by a resistance wire, wound on the ceramic work tube, which is an integral part of the furnace. The annealing temperature was measured by a thermocouple inserted in the middle of furnace. The albite samples were loaded on an alumina boat. The temperature of 1076 °C was chosen as within the field of thermodynamically disordered albite, just a few degrees below melting, at 1100 °C [1]. Annealing duration, with wavenumber and linewidth of the studied peaks, are reported in Table 1.

2.2 Single crystal X-ray Diffraction

Single crystals of albite (all approximately 0.3 x 0.3 x 0.2 mm^3), free of zoning, twinning or inclusions under a polarized microscope, were picked for the X-ray diffraction measurements from the annealed samples. X-ray intensity data were collected at 298 K and up to $2\theta_{max} \sim 72°$ with a Xcalibur 4-circle diffractometer at the Earth Sciences Department, University of Milan, equipped with CCD and monochromatized Mo*K*α radiation, operated at 50 kV and 40 mA. The data collections were performed with a combination of ω and φ scans, fixing a step size of 1° and a time of 10 s for each frame. The diffraction patterns were all indexed with a *C*-centered lattice as reported in the literature (for the untreated sample we obtained: *a*=8.1395(5) Å, *b*=12.7838(7) Å, *c*=7.1597(6) Å, α=94.242(6)°, β=116.59(7)°, and γ=87.674(5)°). The intensity data were then integrated with the computer package CrysAlis (distributed by Agilent on 2013) and corrected for Lorentz-polarization and absorption, by Gaussian integration based upon the physical description of the crystal.

The X-ray intensity data were processed with a series of programs implemented in the WinGX package [13], aimed to provide a check of the statistical distribution of the normalized structure factors (*E*'s). The anisotropic structure refinements were performed with the SHELX-97 software [14] against F^2 and using as starting atomic coordinates those of the structural model of Meneghinello et al. [8]. The neutral X-ray scattering curves of Na, Al, Si and O were used according

to the *International Tables for Crystallography C* [15]. The secondary isotropic extinction effect was modelled according to the Larson's formalism [16], as implemented in the SHELXL-97 package [15]. The first cycles of refinement were conducted with the three independent tetrahedral sites $T_1(o)$, $T_2(o)$ and $T_2(m)$ modeled with the scattering curve of Si and the fourth, *i.e.,* $T_1(m)$,) with the scattering curve of Al. Any attempt to use mixed scattering curves of (Si +Al) did not improve the figures of merit if compared to refinements with the curves of Si and Al alone. For all the refinements, good agreement indexes were obtained (R_1 and wR_{all} in Table S1). Electron density residuals in the difference Fourier map were lower than 0.5 $e^-/Å^3$ in ordered albite before annealing. After annealing, significant electron density residuals were found close to the Na atom, up to 1.3 $e^-/Å^3$ in the longest runs, and the final agreement index increased (R_1, wR_{all}). As the internal R_{int} does not change significantly, the slight increase in the agreement index is not accounted for by a degradation of the crystal, but by Al-Si disorder: the internal disorder does not disrupt the internal lattice, allowing the crystal to remain a crystal. Unit cell and refinement parameters, atomic coordinates and displacement parameters, and selected bond distances are listed in Tables S1, S2 and S3 (Supporting information).

2.3 Raman spectroscopy

Raman spectra were collected with a Jobin Yvon Horiba LabRam confocal spectrometer, equipped with a charge-coupled detector (CCD), using an Olympus BX40 microscope. The beam of a He-Ne laser at 632.8 nm was focused on the sample with a spot diameter of ~ 2 μm (ultra-long working distance objective 50x, NA = 0.55), using a confocal aperture of 150 μm. The spectral resolution was ~ 1.5 cm^{-1}. Before each measurement session, the system was calibrated against the 520.6 cm^{-1} Raman peak of pure silicon. Unpolarized Raman spectra were collected in backscattered geometry in the spectral range 100-1100 cm^{-1}, with 60-120 s counting times and 3-6 accumulations. The peak position was determined, with accuracy better than 0.5 cm^{-1}, by peak fitting, made with LABSPEC 5.78.24 Jobin Yvon/Horiba software package, using pseudo-Voigt profiles, subdividing each spectrum in three spectral ranges. A 2nd degree polynomial curve was subtracted as baseline to remove fluorescence background before peak fitting. All Raman spectra were collected at room temperature.

For each annealing run, the spectra of two different fragments were collected, after cooling at room temperature in air. Eight to twenty spectra were averaged for each run. For each peak position and linewidth (full width at half maximum, FWHM), the average value and the standard error of the mean (SEM) were calculated. Measurements from the same experimental run showed SDs (standard deviations) and SEMs of peak positions not larger than ± 1 cm^{-1} and ± 0.5 cm^{-1},

respectively, for the two most intense Raman bands at 507 and 478 cm^{-1}; they got worse (i.e., ± 1.6 and ± 0.8 cm^{-1}, respectively) for the Raman band at 290 cm^{-1}. As regards peak linewidths, SDs varied between 0.9 and 3.4 cm^{-1}, according to the investigated band and annealing time, and SEMs were in the range 0.3-1.1 cm^{-1}.

The results are an average for the collected spectra (Table 1). Representative Raman spectra with annealing time are shown (Fig. 1).

3. Results

3.1 Single crystal X-ray diffraction and Al-Si order

In ordered albite, Al lies at one of four symmetry independent tetrahedral sites, *i.e.* $T_1(o)$, and Si is confined at the other three sites, $T_2(o)$, $T_2(m)$ and $T_1(m)$. With Al-Si disordering, Al atoms migrate to the other sites, and in fully disordered albite each site is occupied by the same amount of Al, *i.e.*, 0.25 atoms per site. A quantitative assessment of the disordering process is obtained by the "order parameter" $Q_{od} = (Al)_{Al} - (Al)_{Si}$, where $(Al)_{Al}$, is the average fractional occupancy of Al at the Al-rich sites, and $(Al)_{Si}$ is the average fractional occupancy of Al at the Si-rich sites [7]. An order parameter Q_{od} may be given directly in terms of bond lengths, assuming a linear relationship between the average tetrahedral bond distances (T-O) and site occupancies:

$$Q_{od} = \langle Al\text{-}O \rangle - \langle Si\text{-}O \rangle)/K \qquad (1)$$

where ⟨Al-O⟩ is the mean bond length of the Al bearing $T_1(o)$ site, and ⟨Si-O⟩ the mean of the bond lengths of the three Si bearing sites; K corresponds to the difference between the same distances in the fully ordered case, and was calibrated by Angel et al. [7] to be 0.135 Å. The order parameter varies between 1 in fully ordered to 0 in fully disordered albite.

Q_{od} for our samples was calculated from the average bond lengths obtained by single crystal X-ray refinements following eqn. 1. As expected, the results were linearly related with the cos γ (being γ one of unit-cell angles) (Fig. 2). In fact, cos γ is very close to the x_6 off diagonal component in the spontaneous strain, which is known to change in response to the Al-Si order ($x_6 = b \cos \gamma / b_0 \sim \cos \gamma$) [17,18], and provides an alternative, albeit indirect, way of measuring the Q_{od}, which confirms the single crystal results.

The displacement parameters of the tetrahedral sites increase in magnitude with the respective bond distances, in response to the increased positional disorder within the tetrahedral site (Fig. 3). Also, the atomic displacement parameters of the Na site increase with the disorder, up to a saturation at $Q_{od} \sim 0.2$ (Fig. 3). The residuals of the electron density close to the Na site increase in response to

positional disorder at the non-tetrahedral site. In ordered albite, Na is present at a single site, weakly bonded and with large thermal ellipsoid [19,20]. In disordered albite, local electrostatic minima appear within the non-tetrahedral cavity where Na is hosted, indicating positional disorder. Positional disorder of Na accounts for larger anharmonic displacement parameters, with local residuals close to the center of gravity of the Na site [21-23].

3.2 Al-Si order and evolution of the Raman peaks

Significant Raman peak broadening occurs during annealing (Figure 1). Some peaks disappear or become hardly detectable (Fig. 1). Peak broadening reflects the change in Al-Si order: the crystals maintain a good quality throughout the annealing, as shown by the low values of the agreement factor between equivalent reflections (R_{int}, Table S1), a parameter which in crystallography can be related to sample degradation. Also peak positions change somewhat with annealing.

To note, different peak broadening was also observed in Raman spectra collected from the same experimental run, i.e. after the same annealing. It was likely caused by inter-crystalline inhomogeneity, i.e., by the presence of internally homogeneous crystals with different degrees of disorder coexisting in the polycrystalline sample. Similar results were found by Meneghinello *et al.* [8] in powder patterns of Stintino albite crystals, heated in the range 1050-1090 °C for different times. The absolute intensities observed in our spectra changed according to the crystallographic orientation of the sample with respect to the polarization of the laser beam.

We expect peak broadening to be related to structural deformational mechanisms occurring with Al-Si ordering, which involves local framework deformation. In their investigation on Al-Si ordering by IR spectroscopy, Wruck *et al.* [4] showed that changes in peak position $\Delta\omega$ and in linewidth $\Delta\Gamma$ are related to the degree of Al-Si order simply by $\Delta\omega \propto \Delta\Gamma \propto Q_{od}^2$: the relation was checked for an infrared active band at 620 cm^{-1} and confirmed on other peaks. Here $\Delta\Gamma$ is the difference $\Gamma-\Gamma_0$ in linewidth of a Raman peak between partially disordered one (Γ) and in in fully ordered albite (Γ_0). The $\Delta\Gamma \propto Q_{od}^2$ relation can be recast as $Q_{od}^2 = a - b\Gamma_0 + b\Gamma$. $a - b\Gamma_0$ is a constant, thus allowing Q_{od}^2 to be calculated from the linewidth of the peaks.

To constrain the relations between peak position, linewidth and the degree of order in Raman spectra, we have selected three strong peaks: 290 cm^{-1} (ν_c), 478 cm^{-1} (ν_b) and 507 cm^{-1} (ν_a). They were all ascribed [5,24] to bending motions in the tetrahedral framework. Tetrahedral stretching modes, at higher energy, are too weak to be used for a calibration.

The linewidth in ordered albite for the three peaks ν_c, ν_b and ν_a is ~7 cm^{-1} and increases with annealing, up to 24, 16 and 12 cm^{-1}, respectively (Fig. 4). The peaks broaden mostly in the first stages, with little increase for longer annealing (Fig. 4). The relation $\Gamma \propto Q_{od}^2$ indicates that the

process probed by peak broadening is indeed that of Al-Si disorder (Fig. 5). Incidentally, high-temperature in situ experiments, in which cation disorder is kinetically inhibited, show peak broadening too, but, differently from cation ordering, the ν_a peak broadens with temperature more than the ν_c peak [11].

An effect of the changes occurring with cation disorder is also evident in the ν_c and ν_b peak positions, which decrease with annealing by 7 and 3 cm^{-1}, respectively. In contrast, the ν_a peak shifts to a higher value by 1.5 cm^{-1}, almost within the experimental error. Peak position and linewidth are related, indicating that peak positions also record significant information (Fig. 6). The relation between the changes in peak position and changes in linewidth is linear only up to 32 days annealing, where the disorder is almost complete. For longer annealing a saturation in linewidth occurs. As linewidth is related to Al-Si order (Fig. 5), we find that peak position (and similarly peak difference) can be related to Al-Si order only up to saturation in linewidth. Further changes in peak position could be related to stoichiometric changes, possibly to Na loss [24].

4. Discussion

4.1 Peak position, linewidth and spontaneous strain

Al-Si disorder affects peak shift and broadening differently in the studied Raman peaks. The ν_a peak broadens less than ν_b and ν_c and increases its wavenumber with disorder. The ν_b and ν_c peaks instead red-shift with disorder, but to a different extent; moreover, the ν_c peak broadens more than ν_a and ν_b (Fig. 6).

As shown above, peaks showing higher difference between peak positions in ordered and disordered configurations show also higher peak broadening. For instance, the ν_a peak, which shows only a slight shift between ordered and disordered albite, shows also less pronounced broadening. We suggest that the structure deformation caused by Al-Si disorder is related to this difference.

Al-Si disorder causes significant changes in the framework geometry, which are revealed by a deformation in the unit cell. The directions of compression or expansion of the unit cell with ordering will decrease or increase anisotropically, triggering a coupling with the Raman modes and the resulting peak positions, as found for instance in the high-pressure behaviour of low albite [25].

In response to the disordering, *a* and *b* unit-cell parameters increase by 0.3 and 0.7%, respectively, whereas the *c*-parameter decreases by 0.7% (Table S1). The peak ν_a at 507 cm^{-1}, which is reported as a vibration of the tetrahedral cages along *c* [24], is the most affected by the compression along the *c* axis. This peak slightly blue-shifts with increasing disorder, i.e., goes to higher wavenumbers. The peak ν_b at 478 cm^{-1}, which is a vibration onto the *a*-*b* plane [26], *i.e.*, the plane where strong expansion occurs, red-shifts (Fig. 6).

Moreover, quantum mechanical calculations have shown that the mode at 507 cm^{-1} (ν_a) is not affected by changing the mass of the substituting cation at the tetrahedral site. Therefore, it is expected to be unchanged for any Al-Si ordering, but for the unit cell compression along the *c* axis, which possibly accounts for the small increase in the wavenumber [5]. The quantum mechanical calculations also show that the mode at 478 cm^{-1} (ν_b) is downshifted (i.e. redshifts) by the substitution of Si with a cation with minor mass, like Al in the tetrahedral site.

Incidentally we note that similar band broadening related to Al/Si disorder (and associated orientational disorder of SiO_4 tetrahedron) is observed in mullite/sillimanite. Al-O bond being more ionic than Si-O one, the spectrum reflects only SiO_4 species contribution and hence is very sensitive to the orientational disorder [27].

4.2 Implications and conclusions

The different behaviour of the Raman active peaks in response to different Al-Si disorder provides useful hints in the investigation of natural plagioclase. The strongest peaks in plagioclase are found at 478 and 507 cm^{-1} (ν_b and ν_a). The ν_a peak is modified less by changing Al-Si order, but more with composition [6, 28]. It is therefore most suitable to assess the compositional changes in plagioclase. On the other hand, the peaks ν_c and ν_b are most suitable to determine the degree of Al-Si order in a given feldspar.

An obvious application of the experimental findings of this study is to determine whether a crystal of albite (or plagioclase) is or not homogeneous in the degree of order, for instance in a metamorphic albite, which was re-heated after crystallization. In spite of the potential information in Al-Si order in albite, only the study by Kroll and Knitter [29] exploited the potential petrologic applications to model rock cooling paths. In their investigation, Kroll and Knitter took advantage of the strong differences in the angle between the optical axes and in XRD powder patterns with Al-Si order-disorder. However, both optical investigation and XRD do not permit spot analyses. Raman spectroscopy can be performed easily on a thin section, or even on a sample without any specific preparation, so that the Al-Si order can be obtained at the micron scale.

We provide here, on the basis of our experimental findings, two possible equations to determine Q_{od} from the linewidth of the peaks ν_c and ν_b. The equations were calibrated against Q_{od} of the seven samples experimentally measured by single crystal X-ray diffraction. For the ν_c and ν_b peaks the relation between Q_{od}^2 and linewidth Γ of the peaks is then:

$$Q_{od}^2 = 1.40(15)-0.064(8)\Gamma_c \qquad R^2=0.93 \qquad (2)$$

$$Q_{od}^2 = 1.51(23)-0.097(17)\Gamma_b \qquad R^2=0.88 \qquad (3)$$

As peak linewidth is affected to some extent by instrumental features, an alternative approach is to exploit the changes in peak position.

We empirically find that the difference Δ_{ab} between the wavenumbers of the most intense peaks ν_a and ν_b is related with the linewidth of the ν_b peak. We have therefore related Q_{od} to the wavenumber difference Δ_{ab} (Fig. 7). Here, only the runs up to 32 days, where linear relation between the degree of Al-Si order and peak positions was found, were considered (Fig. 6). The Q_{od} was obtained from Γ_b by eqn. 3; the use of eqn, 2 would not affect significantly the results. The change in Δ_{ab} is rather modest (3 cm^{-1}), but still related to Q_{od} through:

$$Q_{od}^2 = 9.50(75) - 0.307(25)\Delta_{ab} \qquad R^2 = 0.94 \qquad (4)$$

The above equation may be useful to calibrate the different degree of order in natural albitic plagioclase, using the two strongest peaks in the Raman spectrum of a plagioclase. The two considered peaks are the most intense, and found in any plagioclase spectrum. The difference between the two peaks is less affected by experimental setup and calibration features, which affect peak broadening and absolute peak position, so that it may be used for an estimate of the degree of order in albite. A check for the above equation can be provided by the Raman data of high albite, where we can assume that Q_{od} is close to 0 [12]. In high albite Δ_{ab} has the value of 31 cm^{-1}, in full agreement with our calibration (Fig. 7).

Acknowledgements

The authors wish to acknowledge the helpful comments of the editor and of two anonymous reviewers.

References

[1] H. Kroll, H.U. Bambauer, U. Schirmer, *Am. Mineral.* **1980**, *65*, 1192.

[2] H. Kroll, P.H. Ribbe, Lattice parameters, composition and Al, Si order in alkali feldspars. Feldspar Mineralogy. (P.H. Ribbe, ed.), Review in Mineralogy, 2, 2nd edition, MSA, **1983**, pp.57-99.

[3] E.K.H. Salje, B. Kuscholke, B. Wruck, H. Kroll, *Phys. Chem. Miner.* **1985**, *12*, 99.

[4] B. Wruck, E.K.H. Salje, A. Graeme-Barber, *Phys. Chem. Miner.* **1991**, 17, 700.

[5] I. Aliatis, E. Lambruschi, L. Mantovani, D. Bersani, S. Andò, G.D. Gatta, P. Gentile , E. Salvioli-Mariani, M. Prencipe, M. Tribaudino, P.P. Lottici, *J Raman Spectrosc.* **2015**, *46*, 501.

[6] D. Bersani D., I. Aliatis, M. Tribaudino, L. Mantovani, A. Benisek, M.A. Carpenter, G.D. Gatta, P.P. Lottici, *J .Raman Spectrosc*. **2018**, doi:10.1002/jrs.5340

[7] R.J. Angel, M.A. Carpenter, L.W. Finger, *Am Mineral.* **1990,** *75*, 150.

[8] E. Meneghinello, A. Alberti, G. Cruciani, *Am. Mineral.* **1999**, *84*, 1144.

[9] W.H. Yang, R.J. Kirkpatrick, D.M. Henderson*, Am. Mineral.* **1986**, *71*, 712.

[10] E.K.H. Salje, B. Guttier, C. Ormerod, *Phys. Chem. Miner.* **1989**, *16*, 576.

[11] E.K.H. Salje, *Phys. Chem. Miner.* **1986,** *13*, 340.

[12] J.J. Freeman, A. Wang, K.E. Kuebler, B.L. Jolliff, L.A. Haskin, *Can. Mineral.* **2008**, *46*, 1477.

[13] L.J. Farrugia, *J. Appl. Crystallogr*. **1999**, *32*, 837.

[14] G.M. Sheldrick, *Acta Crystallogr*. A **2008**, *64*, 112.

[15] A.J.C. Wilson, E. Prince, Eds. International Tables for X-ray Crystallography, Volume C: Mathematical, physical and chemical tables (2nd Edition), **1999**, Kluwer Academic, Dordrecht, NL.

[16] A.C. Larson, *Acta Crystallogr. A,* **1967**, *23*, 664.

[17] E.K.H. Salje*, Phys. Chem. Miner*. **1985,** *12*, 93.

[18] M.A. Carpenter, E.K.H. Salje, A. Graeme-Barber, *Eur. J. Mineral.* **1998,** *10*, 621.

[19] J.K. Winter, S. Ghose, F.P. Okamura, *Am. Mineral.* **1977**, *62*, 921.

[20] J.V. Smith, G. Artioli, Å. Kvik, *Am. Mineral*. **1986**, *71*, 727.

[21] C. T. Prewitt, S. Sueno, J.J. Papike, *Am. Mineral.* **1976**, *61*, 1213.

[22] J.K. Winter, F.P. Okamura, S. Ghose, S. *Am. Mineral*. 1**979**, *64*, 409.

[23] J. E. Post, C.W Burnham, *Am. Mineral*. **1987**, *72*, 507.

[24] L. Johnson, R.A. McCauley, *Thermochim. Acta* **2005**, *437*,134

[25] I. Aliatis, E. Lambruschi, L. Mantovani, D. Bersani, G.D. Gatta, M. Tribaudino, P.P. Lottici, *Phys. Chem. Miner*. **2017**, *44*, 213.

[26] D.A. McKeown, *Am. Mineral.* **2005**, *90*, 1506.

[27] D. Michel, Ph. Colomban, S. Abolhassani, F. Voyron, A. Kahn-Harari, *J Eur Ceramic Soc*, **1996**, *16*, 161

[28] K. S. Befus, J. F. Lin, M. Cisneros, S. Fu, *Am. Mineral.*, **2018**, *103*, 600.

[29] H. Kroll, R. Knitter, *Am. Mineral*. **1991**, *76*, 928.

Table 1: peak position ν and linewidth (FWHM) in cm^{-1} of the major peaks for albite at different annealing. Standard Deviations (SD) and Standard Error on the Mean (SEM) are discussed in the text.

t (days)	ν_b	FWHM		ν_a	FWHM		ν_c	FWHM	
0	479.1	7.1		507.4	7.3		290.6	8.0	
4	478.7	9.1		507.3	9.5		289.3	11.2	
8	478.0	11.7		507.5	11.0		288.3	15.2	
11	477.2	10.7		506.5	11.1		287.6	14.3	
12	477.7	13.5		507.4	11.6		288.3	15.6	
16	476.9	14.5		507.5	12.3		284.8	21.6	
20	477.9	14.0		508.3	12.2		286.2	20.4	
25	477.7	13.0		507.5	12.0		286.5	18.9	
28	477.6	15.5		508.4	12.4		285.0	22.0	
32	476.8	15.2		507.7	12.6		284.8	20.9	
35	478.1	15.3		508.7	12.3		285.9	21.1	
38	476.4	17.6		508.5	13.0		283.0	22.2	
40	476.5	16.7		508.0	12.9		283.5	22.0	
42	476.4	16.3		507.3	12.9		283.9	23.0	
46	476.5	16.5		507.5	13.0		283.3	24.1	

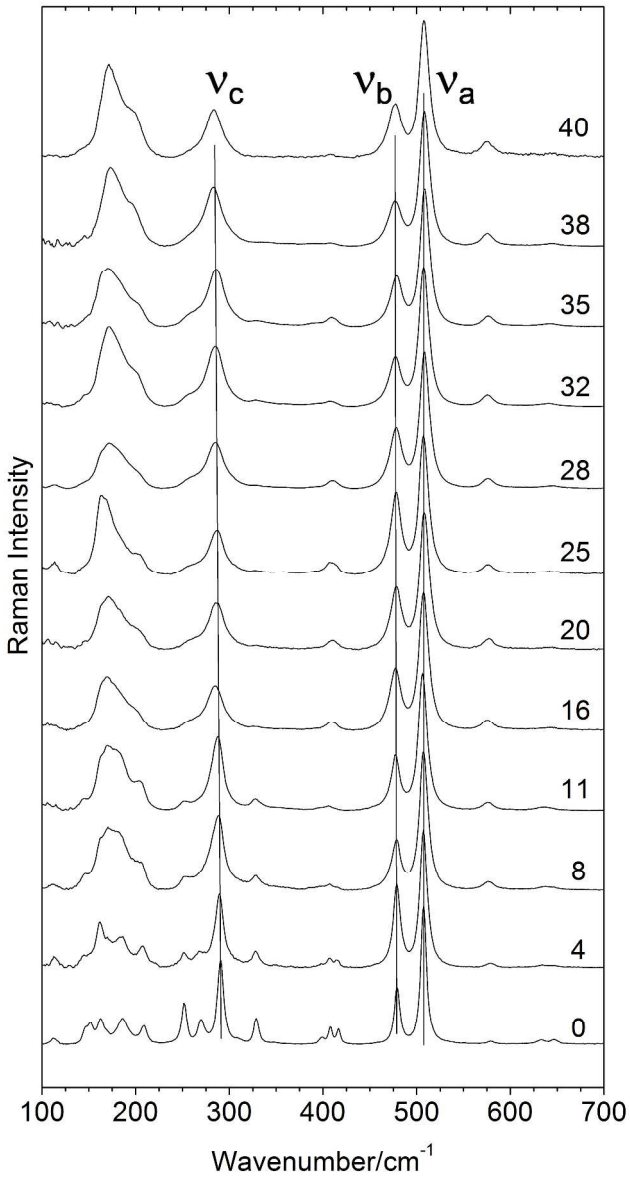

Figure 1: representative Raman spectra for annealed albite: full spectra with annealing time (in days)

301x509mm (300 x 300 DPI)

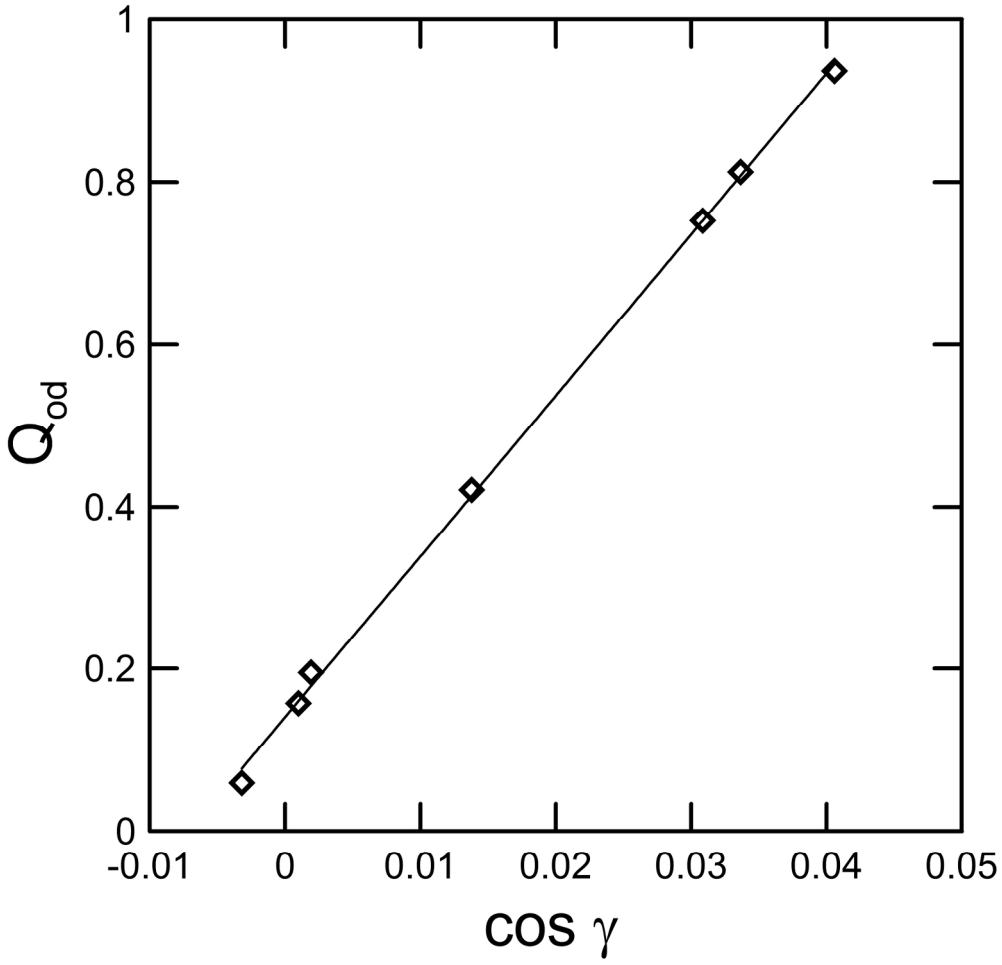

Figure 2: long range order parameter Q_{od} from SCXRD vs cos γ. The error is within the size of the symbol.

180x172mm (300 x 300 DPI)

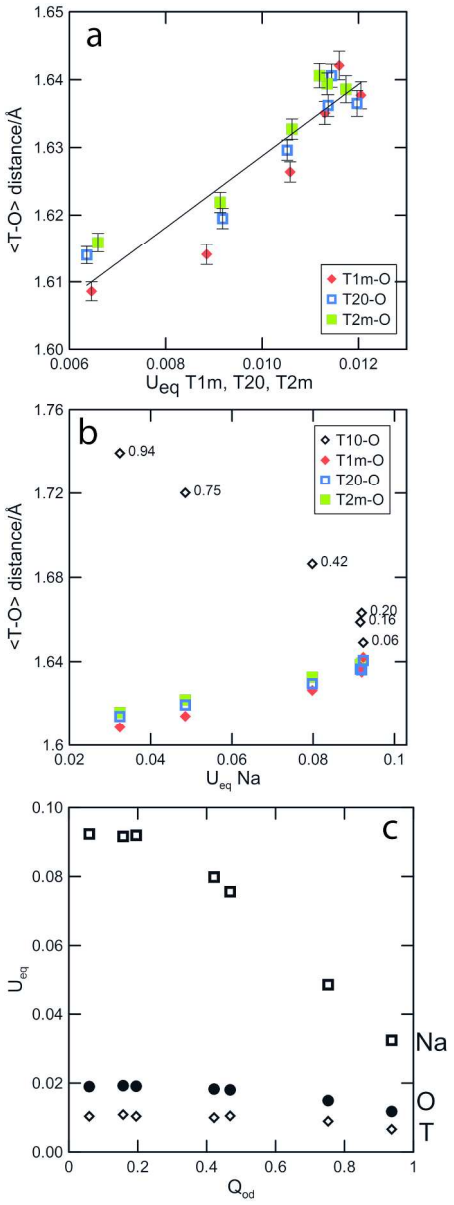

Figure 3: a) tetrahedral bond distances vs displacement parameters (Å^2) of atoms in the T1(m), T2(o) and T2(m) sites; b) tetrahedral bond distances [Q_{od} value is shown near the T1(o) Al centred tetrahedron] vs displacement parameter of the non-tetrahedral sodium; c) displacement parameters of Na, O and T sites vs Q_{od} (the grand mean for O and T sites is reported). When not shown, the error is within the size of the symbol.

100x271mm (300 x 300 DPI)

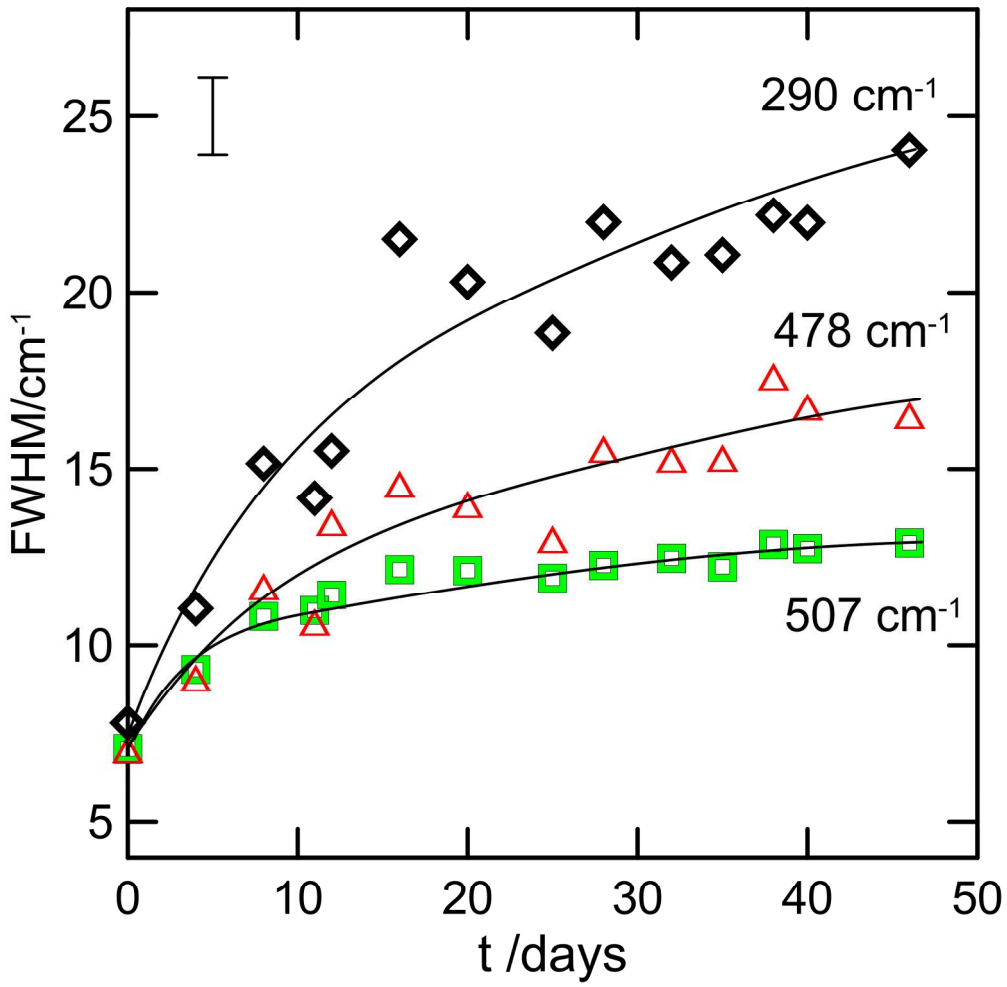

Figure 4: linewidth of the main peaks vs annealing time. Continuous black lines are provided to aid the eye. The error bar gives the maximum standard error of the mean.

179x175mm (300 x 300 DPI)

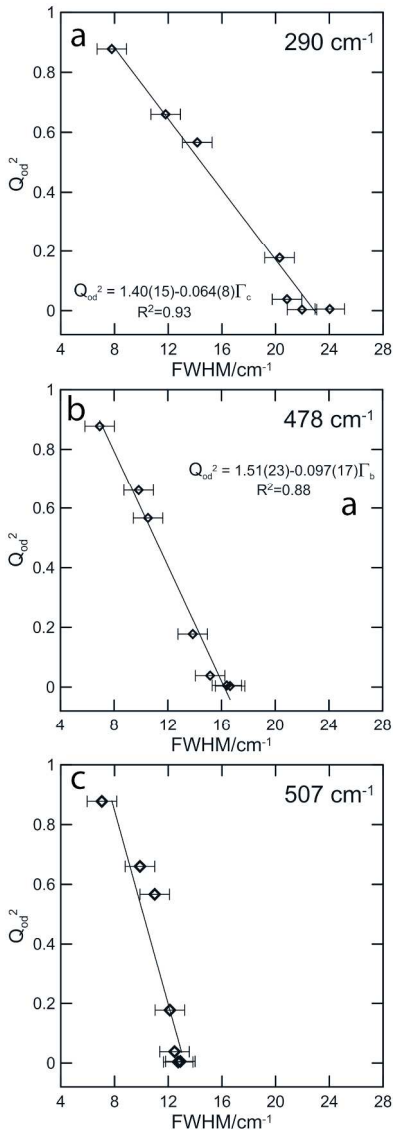

Figure 5: Q_{od}^2 vs absolute linewidth for the peaks at a) 290 cm^{-1} (v_c); b) 478 cm^{-1} (v_b) and c) 507 cm^{-1} (v_a). The equations of the linear fits for v_c and v_b, are reported in the discussion as Eqs. (2) and (3), respectively.

91x285mm (300 x 300 DPI)

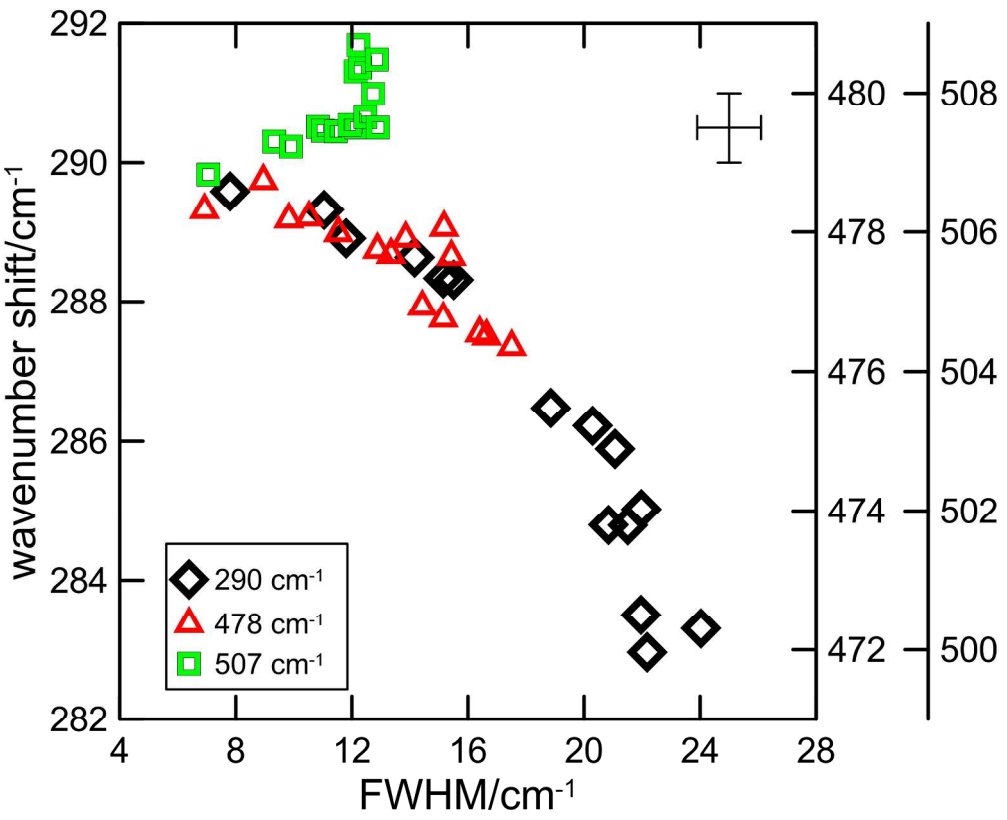

Figure 6: Raman shift vs linewidth for the main peaks at 290 cm^{-1} (v_c), 478 cm^{-1} (v_b) and 507 cm^{-1} (v_a). The error bars indicate the maximum error on the mean for the given spectra.

219x178mm (300 x 300 DPI)

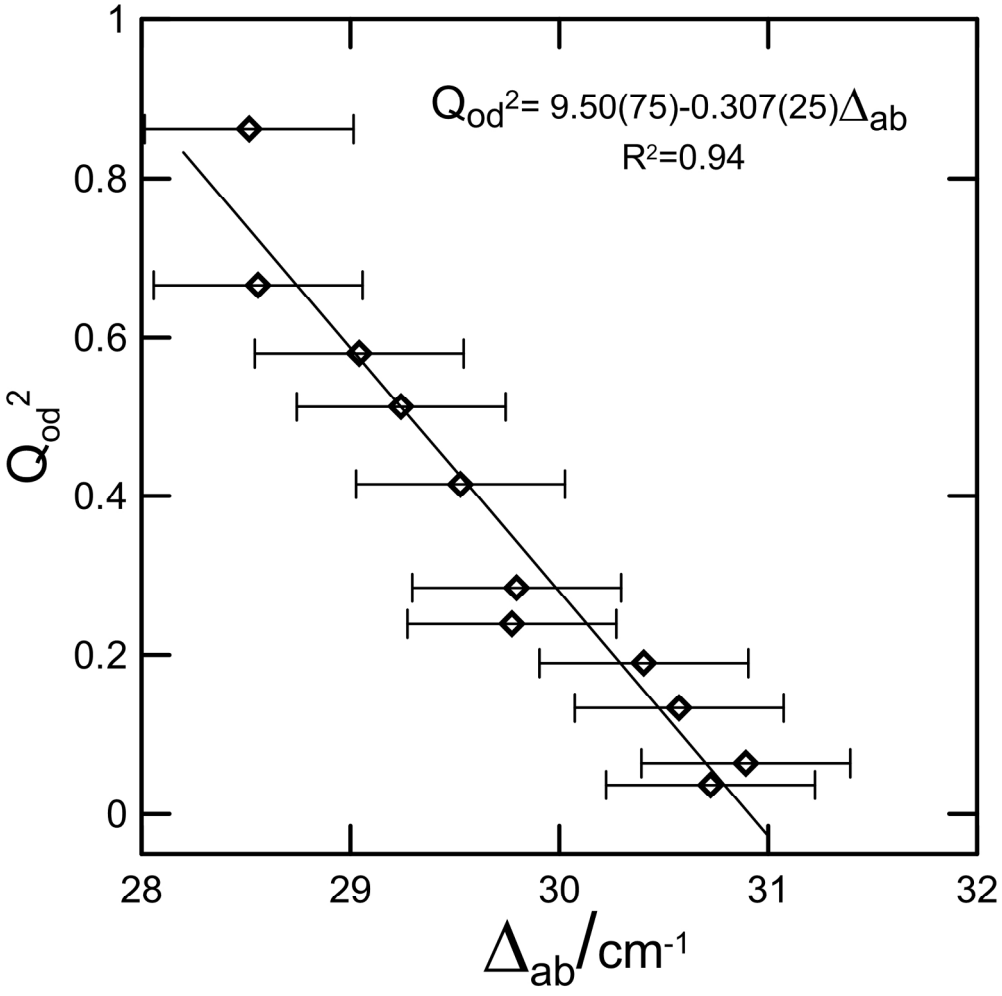

Figure 7: Q_{od}^2 vs wavenumber difference between peaks v_a and v_b.

182x181mm (300 x 300 DPI)